Critical fields, thermally activated transport, and critical current density of β-FeSe single crystals

Hechang Lei (雷和畅), Rongwei Hu (胡荣伟), and C. Petrovic

Critical fields, thermally-activated transport and critical current density of β-FeSe single crystals

Hechang Lei (雷和畅), Rongwei Hu (胡荣伟),[*] and C. Petrovic
Condensed Matter Physics and Materials Science Department,
Brookhaven National Laboratory, Upton, NY 11973, USA

We present critical fields, thermally-activated flux flow (TAFF) and critical current density of tetragonal phase β-FeSe single crystals. The upper critical fields $H_{c2}(T)$ for H∥(101) and H⊥(101) are nearly isotropic and are likely governed by Pauli limiting process. The obtained large Ginzburg-Landau parameter $\kappa \sim 72.3(2)$ indicates that β-FeSe is a type-II superconductor with smaller penetration depth than in Fe(Te,Se). The resistivity below T_c follows Arrhenius TAFF behavior. For both field directions below 30 kOe single vortex pinning is dominant whereas collective creep becomes important above 30 kOe. The critical current density J_c from M-H loops for H∥(101) is about five times larger than for H⊥(101), yet much smaller than in other iron-based superconductors.

PACS numbers: 74.70.Xa, 74.25.Op, 74.25.Wx, 74.25.Sv

I. INTRODUCTION

Among iron-based superconductors, the tetragonal β-FeSe has trigged great interest because of simplest structure and superconductivity below about 8 K without any carrier doping.[1] Besides β-FeSe, the superconductivity has also been discovered in binary Fe(Te,Se) and Fe(Te,S) materials.[2,3] These materials also have similar Fermi surface to FePn (Pn = P, As)-based superconductors,[4] even though they have FeCh (Ch = Te, Se, S) layers stacked along the c-axis as opposed to FePn layers. Understanding this similarity is rather important. Binary FeCh material, β-FeSe has another notable characteristics. Application of pressure leads to a significant enhancement of T_c up to 37 K at around 9 GPa, the third highest known critical temperature for any binary compound.[5]

In order to study anisotropic and intrinsic physical properties of materials, single crystals are required. When compared to Fe(Te,Se) and Fe(Te,S), extremely complex phase diagram of FeSe makes impurities such as α-FeSe and Fe_7Se_8 ubiquitous in as-grown crystals, or sometimes polycrystals impeding the understanding of β-FeSe.[6−10]

Here, we report intrinsic superconducting properties of β-FeSe single crystals. These include critical fields H_{c2} and H_{c1}, thermally-activated flux flow (TAFF) behavior, and the critical current density J_c. Our results show that β-FeSe is a type-II superconductor with large Ginzburg-Landau parameter κ and smaller critical current density when compared to other iron-based superconductors. Single vortex pinning dominates vortex dynamics below 30 kOe, whereas collective creep becomes important at higher magnetic fields.

II. EXPERIMENT

Details of synthesis and structural characterization are explained elsewhere.[11] Thin Pt wires were attached to electrical contacts made of Epotek H20E silver epoxy for a standard four-probe measurement, with current flowing in crystal plane. Sample geometry were measured with an optical microscope Nikon SMZ-800 with 10 μm resolution. Magnetization and resistivity measurements were carried out in Quantum Design MPMS and PPMS, respectively.

III. RESULTS AND DISCUSSION

Figure 1(a) shows the temperature dependence of the in-plane resistivity $\rho(T)$ below 300 K. The residual resistivity ratio (RRR) of 14 is double that of the hexagonal shape crystals,[6] indicating good sample quality. The curvature of $\rho(T)$ changes at about 100 K (Fig. 1(a) inset (a)) due to structural and magnetic transitions in agreement with previous results.[1,6,12] With further decrease in temperature, superconductivity emerges with $T_{c,onset} \simeq 11.4$ K and $T_{c,0} \simeq 8.1$ K (Fig. 1(a) inset (b)), similarly to reported values in the literature.[6] Fig. 1(b) presents the ac susceptibility of FeSe single crystal for field perpendicular to the crystal plane. The corresponding superconducting volume fraction at T = 1.8 K is about 70 %, confirming the bulk nature of superconductivity. The XRD pattern of a single crystal (Fig. 1(b) inset) reveals that the crystal surface is normal to (101) direction, also similar to previous results.[6,8]

Figure 2 (a) and (b) show temperature dependence of $\rho(T)$ in various fields for H∥(101) and H⊥(101). The T_c shifts to lower temperature without obvious broadening for both directions with the increase in magnetic fields. Temperature dependence of the upper critical fields $H_{c2}(T)$ was determined from the resistivity drops to 90%, 50%, and 10% of the normal-state resistivity ρ_n(T,H) (Fig. 2(c)). The normal-state resistivity was determined by linearly extrapolating the normal-state behavior above the onset of superconductivity. The $H_{c2}(T)$ curves are nearly linear and the initial slopes $dH_{c2}/dT|_{T_c}$ are given in Table 1. The slopes are nearly identical for both field directions and the anisotropy of the upper crit-
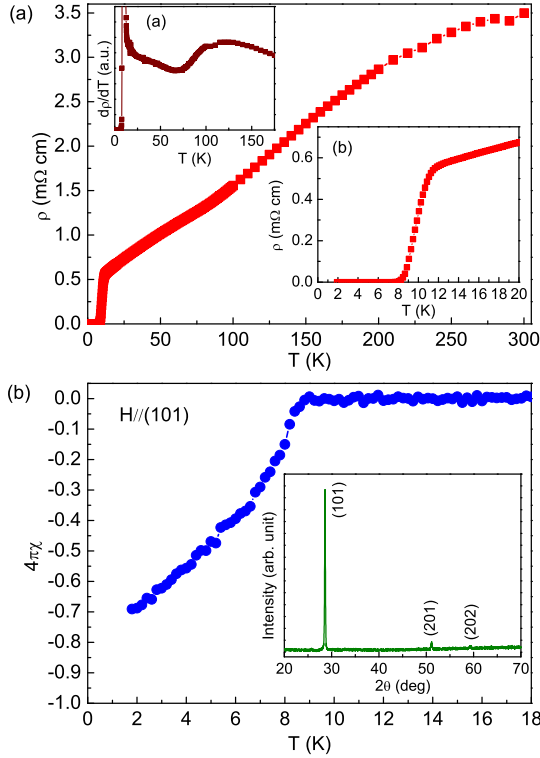
FIG. 1. (a) Temperature dependence of the in-plane resistivity $\rho(T)$ of β-FeSe single crystals. Inset (a) shows derivative of resistivity data $d\rho/dT$ as a function of temperature. Inset (b) shows enlarged resistivity curve near T_c. (b) Temperature dependence of dc magnetic susceptibility of β-FeSe single crystals for H = 10 Oe along the (101) plane. Inset: single crystal XRD pattern of β-FeSe.

FIG. 2. Temperature dependence of the resistivity $\rho(T)$ of β-FeSe single crystals for (a) H(101) and (b) H(101) in the magnetic field up to 90 kOe. (c) Temperature dependence of the resistive upper critical field $H_{c2}(T)$ corresponding to three defined temperatures for both field directions (see text).

ical field $\gamma(T) = H_{c2,H\perp(101)}(T)/H_{c2,H\|(101)}(T)$ is also isotropic within the experimental error.

Within the weak coupling BCS theory[13] and using the slope determined from the midpoint of resistive transition with $T_c = 9.8$ K we can estimate $H_{c2}(0) = -0.693T_c(dH_{c2}/dT|_{T_c}) = 180(4)$ kOe for both field directions. The results are close to the Pauli paramagnetic limit $H_P(0) = 1.84T_c = 180(4)$ kOe.[14] It implies that the spin-paramagnetic effect may be the dominant pair-breaking mechanism in FeSe for both field directions, similar to Fe(Te,Se) and Fe(Te,S).[15,16] The superconducting coherence length $\xi(0)$ estimated using the Ginzburg-Landau formula $H_{c2}(0) = \Phi_0/2\pi\xi^2(0)$, where $\Phi_0 = 2.07\times10^{-15}$ Wb is the flux quantum, is $\xi(0) = 4.28(5)$ nm, which is somewhat larger than Fe(Te,Se) and Fe(Te,S).[15,16]

According to the thermally-activated flux flow (TAFF) theory, the $ln\rho - 1/T$ in TAFF region can be described using Arrhenius relation,[17,18]

$$ln\rho(T,H) = ln\rho_0(H) - U_0(H)/T \qquad (1)$$

where $ln\rho_0(H) = ln\rho_{0f}+U_0(H)/T_c$ is the temperature-independent constant and $U_0(H)$ is the apparent activated energy. Hence, the $ln\rho(T,H)$ vs. $1/T$ should be
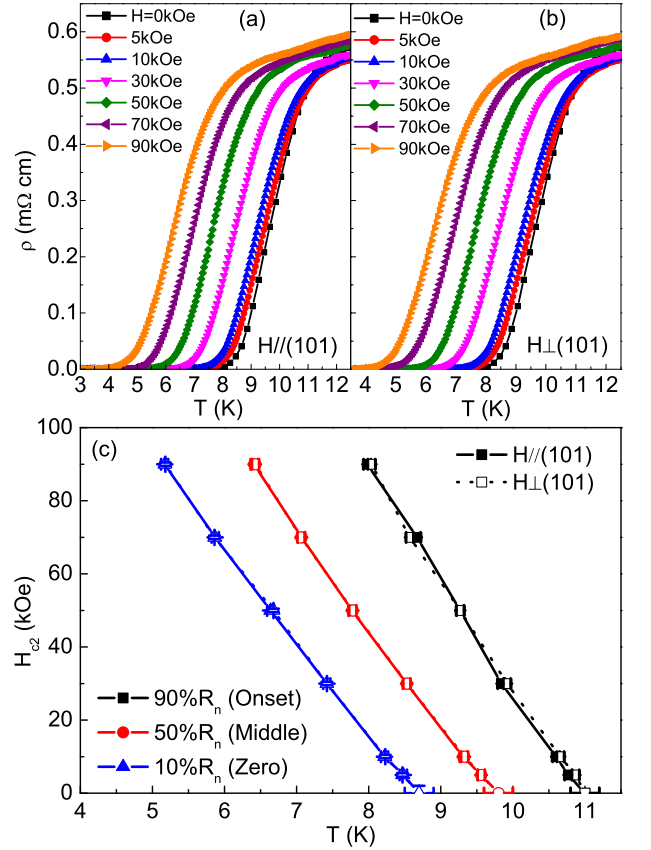
linear in TAFF region. As shown in Fig. 3 (a) and (b), the Arrhenius relation (solid lines) can fit the experimental data very well for both field directions. The results are shown in the common logarithmic scale in the figures, but we calculate them in the natural one. The obtained U_0 are similar for both field directions. They are comparable to that in Fe(Te,S) and much smaller than in Fe(Te,Se).[19,20] The good linear behavior indicates that the temperature dependence of thermally activated energy (TAE) $U(T,H)$ is approximately linear, i.e., $U(T,H) = U_0(H)(1 - T/T_c)$.[17,18] The $\log\rho(T,H)$ lines for different fields extrapolate to the same temperature T_{cross}, which should equal to T_c.[19] The extrapolated temperatures are about 11.1 K for both H$\|$(101) and H$\perp$(101). Moreover, $ln\rho_0(H) - U_0(H)$ show linear behavior for both field directions (Fig. 3(c)). Fits using $ln\rho_0(H) = ln\rho_{0f} + U_0(H)/T_c$, yielded values of ρ_{0f} and T_c 37(1) $m\Omega \cdot cm$ and 11.2(1) K for H$\|$(101) and 39(2) $m\Omega \cdot cm$ and 11.2(1) K for H$\perp$(101). The T_c values are consistent with the values of T_{cross} within the error bars. The $U_0(H)$ shows a power law $(U_0(H) \sim H^{-\alpha})$ field dependence for both directions (Fig. 3(d)). For H$\|$(101), $\alpha = 0.25(6)$ for H < 30 kOe and $\alpha = 0.68(6)$ for H > 30 kOe; For H$\perp$(101), $\alpha = 0.26(2)$ for H < 30 kOe and $\alpha = $

TABLE I. Superconducting parameters of β-FeSe.

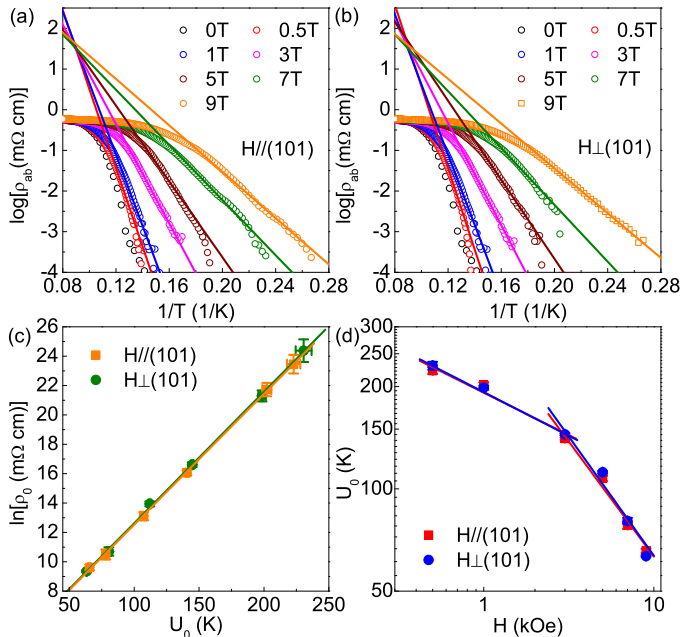|	$T_{c,mid}$ (K)	$(dH_{c2}/dT)_{T_c}$ (kOe/K)			$H_{c2,mid}(0)$ (kOe)	$\xi(0)$ (nm)	$H_P(0)$ (kOe)	$H_{c1}(0)$ (Oe)	$\lambda(0)$ (nm)	$H_c(0)$ (kOe)	$\kappa(0)$
		Onset	Middle	Zero							
H∥(101)	9.8(2)	-30.3(6)	-26.5(6)	-25.4(4)	180(4)	4.28(5)	180(4)	75(2)	309(4)	1.76(3)	72.3(2)
H⊥(101)	9.8(2)	-29.6(6)	-26.6(6)	-25.5(4)	180(4)	4.28(5)	180(4)				

FIG. 3. Log$\rho(T,H)$ vs. $1/T$ in various field for (a) H∥(101) and (b) H⊥(101). The corresponding solid lines are fitting results from the Arrhenius relation. (c) $ln\rho_0(H)$ vs. $U_0(H)$ derived from Arrhenius relation for both field directions. The solid lines are linear fitting results. (d) Field dependence of $U_0(H)$. The solid lines are power-law fitting using $U_0(H) \sim H^{-\alpha}$.

FIG. 4. Low field M(H) of β-FeSe single crystals at various temperatures for (a) H∥(101) and H⊥(101). (c) Temperature dependence of $H_{c1}(T)$ for both field directions. The solid line is the fitted lines using $H_{c1}(T) = H_{c1}(0)[1-(T/T_c)^2]$ for H∥(101).

0.70(9) for H > 30 kOe. The weak power law decreases of $U_0(H)$ in low fields for both field directions implies that single-vortex pinning dominates in this region,[21] followed by a quicker decrease of $U_0(H)$ in field which could be related to a crossover to a collective flux creep regime.[22]

Low field M(H) at various temperatures for H∥(101) and H⊥(101) are shown in Fig. 4(a) and (b), respectively. All curves exhibit linear behavior for low fields and then deviate from linearity at different field values for different temperatures. The values of H_{c1} are determined by examining the point of deviation from the linear slope of the magnetization curve. The temperature dependence of $H_{c1}(T)$ for both field directions are shown in Fig. 4(c). For H∥(101), the $H_{c1}(T)$ can be well fitted using the formula $H_{c1}(T) = H_{c1}(0)[1-(T/T_c)^2]$ and the obtained $H_{c1,H\parallel(101)}(0)$ is 75(2) Oe. For H⊥(101), it is difficult to estimate the $H_{c1,H\perp(101)}(T)$ and obtain reliable fits. This is due to the small obtained value for H_{c1} with relative large error and significant demagnetization
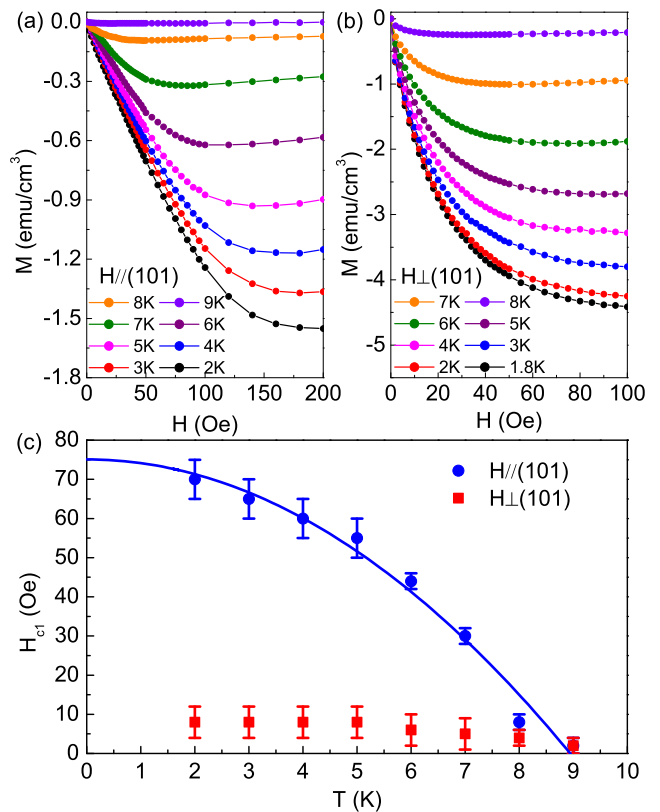
factors.

Since Fe(Te,Se) and Fe(Te,S) superconductors are in the dirty limit, we assume the same for FeSe.[23] Using estimated values of $H_{c1,H\parallel(101)}(0)$, $H_{c2}(0)$ and $\xi(0)$, we evaluate additional parameters using expressions $H_{c2}(0) = \sqrt{2}\kappa H_c(0)$ and $H_{c1}(0) = \frac{H_c(0)}{\sqrt{2}\kappa}(\ln\kappa + 0.08)$ where $\kappa = \lambda/\xi$ is the Ginzburg-Landau (GL) parameter and $H_c(0)$ is the thermodynamic upper critical field at T = 0 K.[24] We obtain $\kappa_{H\parallel(101)}(0) = 72.3(2)$, $H_{c,H\parallel(101)}(0) = 1.76(3)$ kOe, and penetration depth for H∥(101) $\lambda_{H\parallel(101)}(0) = 309(4)$ nm which is somewhat smaller than in Fe(Te,Se).[23] All superconducting parameters are listed in Table 1.

Figures 5(a) and (b) show isothermal magnetization curves M(H) at various temperatures for H∥(101) and H⊥(101). The shape of the M(H) curves confirms that
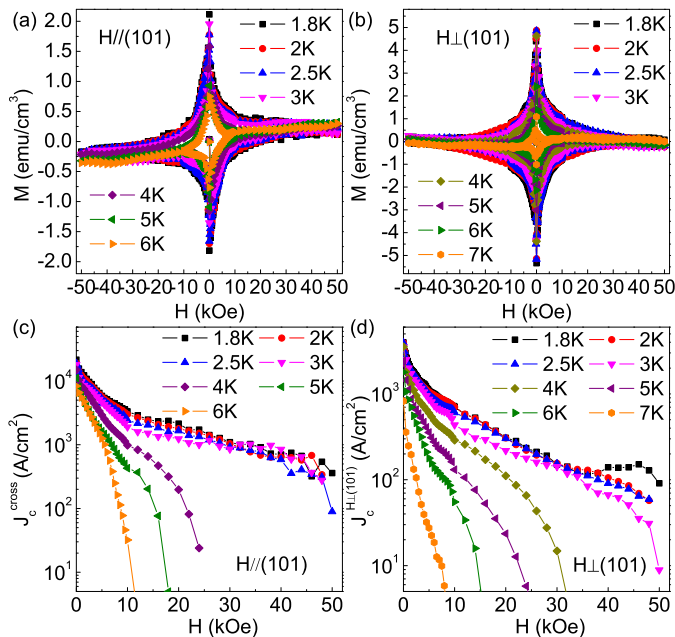
FIG. 5. M(H) loops of β-FeSe single crystals at various temperatures with field up to 50 kOe for (a) H∥(101) and H⊥(101). (c) In-plane and (d) interplane superconducting critical currents as determined from magnetization measurements using the Bean model.

β-FeSe is a typical type-II superconductor. The data exhibit a central peak at zero magnetic field and then the magnetization decreases continuously with increasing magnetic field. On the other hand, there is a weak ferromagnetic (WFM) background superimposed on the superconducting M(H) curve for H∥(101). This WFM background possibly arises due to vacancy-induced magnetic cluster.[11] From the irreversible parts of the M(H) loops, the critical current can be determined using the Bean model.[25,26] For a rectangular-shaped crystal with dimension c < a < b, when H⊥(101), the in-plane critical current density $J_c^{H\perp(101)}(H)$ is given by $J_c^{H\perp(101)}(H) = 20\Delta M(H)/[a(1 - a/3b)]$, where a and b (a < b) are the in-plane sample sizes, $\Delta M(H)$ is the width of the magnetic hysteresis loop in emu/cm^3. On the other hand, for H∥(101), there are two different current densities: the vortex motion across the planes, $J_c^{cross}(H)$ and that parallel to the planes, $J_c^{para}(H)$. As-

suming $a, b \gg (c/3) \cdot J_c^{para}(H)/J_c^{cross}(H)$,[26] we obtain $J_c^{cross}(H) \approx 20\Delta M(H)/c$. The magnetic field dependence of $J_c^{cross}(H)$ and $J_c^{H\perp(101)}(H)$ is shown in Fig. 4(c) and 4(d), respectively. It should be noted that for H∥(101), the WFM background has only minor effect on the calculation of $\Delta M(H)$, because of very weak moment contribution of WFM. The error of calculated $J_c^{cross}(H)$ is about 10% without subtracting WFM background. It can be seen that the $J_c^{cross}(0)$ and $J_c^{H\perp(101)}(0)$ at 1.8 K are about 2.2×10^4 and 4×10^3 A/cm^2, which are much smaller than in Fe(Te,Se) and Fe(Te,S) at the same temperature.[27,28] The ratio of $J_c^{cross}(H)/J_c^{H\perp(101)}(H)$ is about 5.4 at 1.8 K. Moreover, above 4 K, the critical current densities decrease with the applied field more quickly than below 4 K, suggesting that the pinning mechanism may change at 4 K.

IV. CONCLUSION

In summary, we present the superconducting properties of β-FeSe single crystals. The results indicate that the $H_{c2}(T)$ is isotropic and the spin-paramagnetic effect may be the dominant pair-breaking mechanism for H∥(101) and H⊥(101). The calculated GL parameter κ indicates that β-FeSe is a typical type-II superconductor with the large κ. The resistivity exhibits clear Arrhenius TAFF behavior with a crossover from single vortex pinning region to collective creep region for both field directions. On the other hand, the critical current density for field along (101) plane is about five times larger than for field normal to (101) plane but still smaller than in Fe(Te,Se) and Fe(Te,S) at the same temperature.

V. ACKNOWLEDGEMENTS

[1] F. C. Hsu, J. Y. Luo, K. W. Yeh, T. K. Chen, T. W. Huang, P. M. Wu, Y. C. Lee, Y. L. Huang, Y. Y. Chu, D. C. Yan, and M. K. Wu, Proc. Natl. Acad. Sci. USA **105**, 14262 (2008).

[2] K.-W. Yeh, T. W. Huang, Y. L. Huang, T. K. Chen, F. C. Hsu, P. M. Wu, Y. C. Lee, Y. Y. Chu, C. L. Chen, J. Y. Luo, D. C. Yan, and M. K. Wu, EPL **84**, 37002 (2008).

[3] Y. Mizuguchi, F. Tomioka, S. Tsuda, T. Yamaguchi, and Y. Takano, Appl. Phys. Lett. **94**, 012503 (2009).

[4] A. Subedi, L. Zhang, D. J. Singh, and M. H. Du, Phys. Rev. B **78**, 134514 (2008).

[5] S. Medvedev, T. M. McQueen, I. Trojan, T. Palasyuk, M. I. Eremets, R. J. Cava, S. Naghavi, F. Casper, V. Ksenofontov, G. Wortmann, and C. Felser, Nature Mater. **8,** 630 (2009).

[6] S. B. Zhang, X. D. Zhu, H. C. Lei, G. Li, B. S. Wang, L. J. Li, X. B. Zhu, Z. R. Yang, W. H. Song, J. M. Dai, and Y. P. Sun, Supercond. Sci. Technol. **22**, 075016 (2009).

[7] U. Patel, J. Hua, S. H. Yu, S. Avci, Z. L. Xiao, H. Claus, J. Schlueter, V. V. Vlasko-Vlasov, U. Welp, and W. K. Kwok, Appl. Phys. Lett. **94**, 082508 (2009).

[8] B. H. Mok, S. M. Rao, M. C. Ling, K. J. Wang, C. T. Ke, P. M. Wu, C. L. Chen, F. C. Hsu, T. W. Huang, J. Y. Luo, D. C. Yan, K. W. Ye, T. B. Wu, A. M. Chang, and M. K. Wu, Cryst. Growth Des. **9**, 3260 (2009).

[9] E. Pomjakushina, K. Conder, V. Pomjakushin, M. Bendele, and R. Khasanov, Phys. Rev. B **80**, 024517 (2009).

[10] T. M. McQueen, Q. Huang, V. Ksenofontov, C. Felser, Q. Xu, H. Zandbergen, Y. S. Hor, J. Allred, A. J. Williams, D. Qu, J. Checkelsky, N. P. Ong, and R. J. Cava, Phys. Rev. B **79**, 014522 (2009).

[11] R. W. Hu, H. C. Lei, M. Abeykoon, E. S. Bozin, S. Billinge, J. B. Warren, T. Siegrist, and C. Petrovic, Phys. Rev. B **83**, 224502 (2011).

[12] S. Margadonna, Y. Takabayashi, M. T. McDonald, K. Kasperkiewicz, Y. Mizuguchi, Y. Takano, A. N. Fitch, E. Suard, and K. Prassides, Chem. Comm. **43**, 5607 (2008).

[13] N. R. Werthamer, E. Helfand, and P. C. Hohenberg, Phys. Rev. **147**, 295 (1966).

[14] A. M. Clogston, Phys. Rev. Lett. **9**, 266 (1962).

[15] H. C. Lei, R. W. Hu, E. S. Choi, J. B. Warren, and C. Petrovic, Phys. Rev. B **81**, 094518 (2010).

[16] H. C. Lei, R. W. Hu, E. S. Choi, J. B. Warren, and C. Petrovic, Phys. Rev. B **81**, 184522 (2010).

[17] T. T. M. Palstra, B. Batlogg, L. F. Schneemeyer, and J. V. Waszczak, Phys. Rev. Lett. **61**, 1662 (1988).

[18] T. T. M. Palstra, B. Batlogg, R. B. van Dover, I. F. Schneemeyer, and J. V. Waszczak, Phys. Rev. B **41**, 6621 (1990).

[19] H. C. Lei, R. W. Hu, E. S. Choi, and C. Petrovic, Phys. Rev. B **82**, 134525 (2010).

[20] C. S. Yadav and P. L. Paulose, New J. Phys. **11**, 103046 (2009).

[21] G. Blatter, M. V. Feigel'man, V. B. Geshkenbein, A. I. Larkin, and V. M. Vinokur, Rev. Mod. Phys. **66**, 1125 (1994).

[22] Y. Yeshurun and A. P. Malozemoff, Phys. Rev. Lett. **60**, 2202 (1988).

[23] H. Kim, C. Martin, R. T. Gordon, M. A. Tanatar, J. Hu, B. Qian, Z. Q. Mao, R. W. Hu, C. Petrovic, N. Salovich, R. Giannetta, and R. Prozorov, Phys. Rev. B **81**, 180503 (2010).

[24] A. A. Abrikosov, Zh. Eksp. Teor. Fiz. **32**, 1442 (1957).

[25] C. P. Bean, Phys. Rev. Lett. **8**, 250 (1962).

[26] E. M. Gyorgy, R. B. van Dover, K. A. Jackson, L. F. Schneemeyer, and J. V. Waszczak, Appl. Phys. Lett. **55**, 283 (1989).

[27] T. Taen, Y. Tsuchiya, Y. Nakajima, and T. Tamegai, Phys. Rev. B **80**, 092502 (2009).

[28] R. W. Hu, E. S. Bozin, J. B. Warren, and C. Petrovic, Phys. Rev. B **80**, 214514 (2009).